Thickness dependence of the effective damping in epitaxial Fe_3O_4/MgO thin films

S. Serrano-Guisan,[1,a)] Han-Chun Wu,[2] C Boothman,[2] M. Abid,[2,b)] B. S. Chun,[3] I. V. Shvets,[2] and H. W. Schumacher[1]
[1]*Physikalisch-Technische Bundesanstalt, Bundesallee 100, 38116 Braunschweig, Germany*
[2]*School of Physics, Trinity College, Dublin 2, Ireland*
[3]*Department of Materials Science and Engineering, Korea University, Seoul 136-713, Republic of Korea*

(Received 9 August 2010; accepted 29 November 2010; published online 5 January 2011)

The precessional magnetization dynamics of high quality epitaxial magnetite (Fe_3O_4) thin films growth on MgO are investigated by inductive magnetization dynamic measurements in time and frequency domain. An upper bound for the intrinsic Gilbert damping parameter of $\alpha_0 = 0.037 \pm 0.001$ is derived, which is significantly lower than previously reported for epitaxial Fe_3O_4 on GaAs. With increasing film thickness from 5 up to 100 nm a strong increase in the effective damping up to 0.2 is observed which cannot be explained by simple nonuniform spin wave excitations. Possible origins of this effect are discussed. © *2011 American Institute of Physics*. [doi:10.1063/1.3531989]

I. INTRODUCTION

The half-metallic character of magnetite (Fe_3O_4) with a predicted full spin polarization at the Fermi level and its high Curie temperature (~850 K) (Ref. 1) makes it an attractive candidate for a variety of spintronic applications.[2] In addition magnetite is nontoxic thereby enabling a variety of biomedical application.[3] For both fields the magnetization dynamics and especially the dissipation of magnetization precession by Gilbert damping are important: in spintronics the damped precession limits the ultimate speed of device operation, whereas for biomedical applications like, e.g., hyperthermia cancer treatment,[3] the efficient dissipation of energy from external oscillating magnetic fields is also determined by the Gilbert damping parameter. Additionally, Gilbert damping limits spin wave propagation in the emerging field of magnonics.[4] Therefore, magnetization dynamics and damping is presently investigated in a variety of spintronic materials like, e.g., half metallic Heusler compounds.[5] Concerning precessional magnetization dynamics of Fe_3O_4 frequency domain experiments of thin films have been used to determine the film anisotropy.[6–8] More recently time resolved magneto-optical Kerr effect measurements have been carried out on 6 nm thick Fe_3O_4 grown on GaAs to investigate the time resolved precession.[9] The resulting Gilbert damping parameter of $\alpha \approx 0.1$ is more than one order of magnitude larger than typically found for 3*d* ferromagnetic metal thin films.[10] Note, however, that the large lattice mismatch of Fe_3O_4 and GaAs (around −5%, when the Fe_3O_4 cell is rotated by 45° with respect to the GaAs cell in the (100) plane[11]) makes GaAs less suitable for growing high quality epitaxial Fe_3O_4 thin films. Hence, also the Gilbert damping could be extrinsically enhanced compared to high quality epitaxial magnetite thin films.

Here, we report pulsed inductive microwave magnetometry (PIMM) (Ref. 12) and vector network analyzer ferromagnetic resonance (VNA-FMR) (Ref. 13) measurements of the magnetization precession and damping of Fe_3O_4 thin films grown on MgO. The low lattice mismatch of only 0.34% of this system allows to grow high quality fully epitaxial magnetite thin films.[14]

In the low thickness limit a significantly lower effective damping of $\alpha_{eff} = 0.037 \pm 0.001$ is found than previously reported for Fe_3O_4 on GaAs.[9] With increasing film thickness up to 100 nm a strong increase in α_{eff} up to about 0.2 is observed which cannot be explained by simple nonuniform spin wave excitations. Possible origins of this effect are discussed.

II. SAMPLE FABRICATION AND EXPERIMENT SETUP

Fully epitaxial Fe_3O_4 thin films with different thickness (5, 15, 50, 60, 65, and 100 nm) were grown on MgO (001) single crystal substrates using an oxygen plasma assisted molecular beam epitaxy (MBE) (DCA MBE M600, Finland) with a base pressure of 5×10^{-10} Torr. Details of the growth procedure are given elsewhere.[8,15] Reflection high energy electron diffraction (RHEED) was employed to confirm the epitaxial growth and establish the growth mode. The presence of the RHEED intensity oscillations confirms that the films grew in a layer-by-layer mode with a growth rate of 0.3 Å/s. The representative RHEED pattern for the substrate and Fe_3O_4 were recorded in (100) azimuth [Figs. 1(a) and 1(b)]. The patterns for the MgO substrate [Fig. 1(a)] showed vertical lattice rods and sharp Kikuchi lines representative of well ordered and smooth surface. Figure 1(b) shows the RHEED image after the growth of 5 nm Fe_3O_4 film show half-order streaks corresponding to the magnetite unit cell positioned between the locations of MgO RHEED lattice

a)Electronic mail: santiago.serrano-guisan@ptb.de.
b)Present address: IPMC, Ecole Polytechnique Federale de Lausanne, Station 3, CH-1015 Lausanne, Switzerland and King Abdullah Institute for Nanotechnology, King Saud University, Riyadh 11451, Saudi Arabia. Electronic mail: mohamed.abid@epfl.ch.

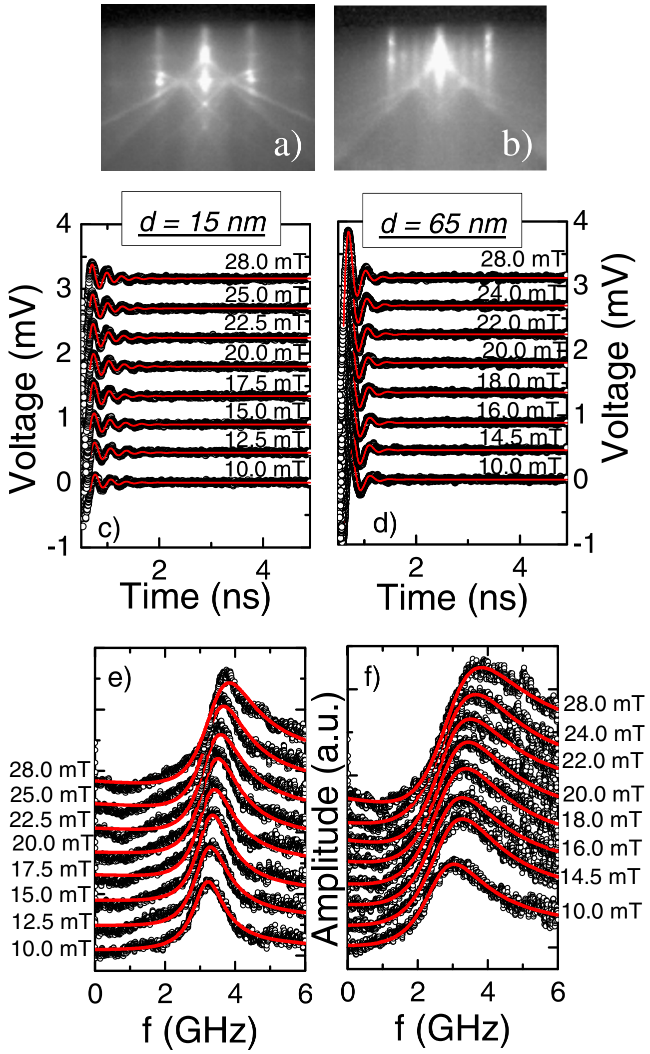

FIG. 1. (Color online) RHEED images of (a) UHV annealed MgO (100) substrate and (b) after 5 nm Fe_3O_4 growth on MgO substrate. The images were recorded in (100) azimuth. PIMM data (c), (d) (black dots) and VNA-FMR data (e), (f) of 15 and 65 nm thick Fe_3O_4 films. Red lines are fits to the data by an exponentially damped sinusoid (c), (d) and a Lorentzian (e), (f), respectively.

rods. This presence of half-order streaks indicates a pseudomorphic growth of magnetite and reflects the double periodicity of its unit cell as compared to MgO. The magnetic behavior of all Fe_3O_4 thin films was examined by means of a physical property measurement system. The in-plane magnetic field was applied along the ⟨001⟩ direction and all films showed a Verwey transition around 120 K, thereby confirming that the magnetite was stochiometric.

For PIMM measurements the Fe_3O_4 films were placed onto a 50 Ω coplanar waveguide connected to a pulse generator and an 18 GHz bandwidth sampling oscilloscope on

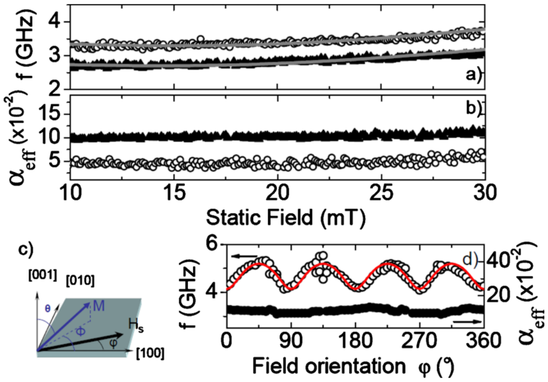

FIG. 2. (Color online) (a) Field dependence of the resonance frequency f of 15 nm (dots) and 65 nm (triangles) thick Fe_3O_4 films. Field is applied along [001]. Solid line is a fit to the dispersion relation. (b) Field dependence of effective damping parameter α_{eff}. (d) Sketch of angular coordinates used in model and experiment. (d) Dependence of f and α_{eff} on in-plane field angle φ at H_S=50 mT. Blue line is a fit to f.

either side.[16] Current pulse application through the waveguide generates a transverse magnetic field pulse (H_p ≈0.2 mT, 100 ps pulse duration) exciting precession of the magnetization M. The induced oscillatory voltage due to precession of the M is captured by the oscilloscope. For frequency domain VNA-FMR measurements, the waveguide is connected to the two ports of the VNA. The harmonic voltage from one port of the VNA excites the precession and the induced voltage amplitude and phase is detected by the other port.

III. RESULTS

Examples of time and frequency domain data for 15 and 65 nm thick films at different static fields are shown in Figs. 1(c)–1(f). PIMM data [(c), (d), open dots] can be well fitted to an exponential damped sinusoid (red lines) indicating small angle precession in the linear regime.[17] VNA-FMR data [(e), (f), open dots] can be well fitted to a Lorentzian function with symmetric and asymmetric component. The FMR frequency f and the effective damping parameter α_{eff} derived from fitting the two data sets are in good agreement.

Figure 2(a) shows the such derived field dependence of f for the two 15 and 65 nm thick films as function of applied field along the [001] orientation. To derive the film parameters the samples are modeled as (001) thin films with a cubic anisotropy field $H_c = 2K_c/M_s$ (with K_c the cubic anisotropy constant and M_s the saturation magnetization), an uniaxial anisotropy field $H_u = 2K_u/M_s$ (with K_u the uniaxial anisotropy constant), an out-of-plane demagnetizing field $H_d = 4\pi M_s$, an in-plane external field H_s, and the easy axis along the ⟨100⟩ directions (see inset in Fig. 2). The resulting dispersion relation is (see Eq. 5 in Ref. 8)

$$f = \frac{\gamma}{2\pi} \times \sqrt{[H_s \cos(\phi-\varphi) + H_c \cos 4\phi + H_u \cos 2\phi] \times \left[H_s \cos(\phi-\varphi) + H_d + \frac{H_c}{4}(3+\cos 4\phi) - \frac{H_u}{2}(1-\cos 2\phi)\right]} \quad (1)$$

where $\gamma = 1.76 \times 10^{11}$ A m^2/s J is the gyromagnetic ratio and ϕ and φ are the in plane angles of M and H_s, respectively, measured from the [100] orientation [see sketch in (c)]. Fitting the measured f to this model yields good agreement as shown by the full lines in Fig. 2(a).

TABLE I. Anisotropies and saturation magnetization extracted from fitting the field and angular dependence of f derived from time and frequency domain data. Also M_s derived from SQUID measurements is shown.

d (nm)	$4\pi M_s$, SQUID (kOe)	$4\pi M_s$, inductive (kOe)	H_c (Oe)	H_u (Oe)
5	11.4 ± 2.3	7.6 ± 0.3	-200 ± 5	20 ± 2
15	7.7 ± 0.5	7.4 ± 0.2	-245 ± 15	72 ± 2
50	6.4 ± 0.15	5.4 ± 0.2	-172 ± 7	35 ± 2
60	6.1 ± 0.2	5.2 ± 0.2	-110 ± 10	2 ± 2
65	6.3 ± 0.1	5.5 ± 0.4	-240 ± 6	90 ± 2
100	6.1 ± 0.1	5.2 ± 0.5	-80 ± 15	0 ± 2

Complementary to the measurements at fixed field orientation VNA-FMR measurements at a higher field amplitude of $H_S = 50$ mT under variation in field angle φ have been performed. Figure 2(d) shows the such derived angular dependence of f and α_{eff} for a 60 nm film. α_{eff} only weakly varies with φ. In contrast f strongly oscillates as expected for a thin film with strong cubic anisotropy. Also here, film parameters can be derived from fitting to the dispersion relation (red line).

The physical parameters of all films deduced from such fits are compiled in Table I. The values are in good agreement with previous studies on Fe_3O_4/MgO thin films,[8] with an enhancement of M_s of thinner films. This effect can be ascribed to a noncompensation of spin moments at the surface of the film.[8] Note, however, that the derived M_s is systematically lower that obtained from SQUID measurements.[15] Here, one possible reason might be the surface oxidization of the films between both measurements leading to the formation of a γ-Fe_2O_3 film of up to 1.5–2 nm thickness.[18] This oxidized film would lead to a reduced M_s, especially for thinner samples.

Figure 3 shows the thickness dependence of the effective damping parameter α_{eff}. Both PIMM (black squares) and VNA-FMR (open dots) data are shown and agree well. With increasing film thickness from 5 to 100 nm α_{eff} increases by about a factor of five (from about 0.039 up to about 0.2). The observed thickness dependence of α_{eff} can be well described by a second order polynomial $\alpha_{\mathrm{eff}} = 0.0365 + 5.6 \times 10^{-4} \times d + 1.09 \times 10^{-5} \times d^2$ (with d in nm; red line). When attributing the increase in the effective damping with thickness to extrinsic effects related to the film thickness, an upper limit of the intrinsic Gilbert damping parameter can thus be derived by extrapolation to $d=0$ yielding $\alpha_0 \leq 0.037 \pm 0.001$. It is important to note, that the intrinsic Gilbert damping parameter of our high quality epitaxial magnetite thin films is significantly lower than has been reported for magnetite on GaAs.[9] We ascribe this significant improvement to the reduced lattice mismatch of MgO with respect to Fe_3O_4 [-0.34% (Ref. 14)].

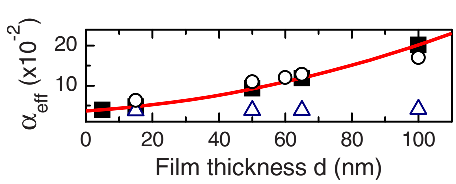

FIG. 3. (Color online) Thickness dependence of the measured effective damping parameter by PIMM (black squares) and VNA-FMR (open dots) by considering saturation magnetization from Table I. Red solid line is a second order polynomial fit. Open triangles show the calculated thickness dependence of α_{eff} by considering non linear spin wave excitation.

IV. DISCUSSION

One possible origin of such thickness dependence could be the generation of spin waves due TO non homogeneous field excitation by the coplanar wave guide.[13] When the magnetic film is much wider than the width of the stripline nonuniform spin wave modes can be excited resulting in a broadened linewidth (and thus an increased α_{eff}). The resulting dependence of α_{eff} on f and d is then given by,[13,19] $\alpha_{\mathrm{eff}} = \alpha_0 + 1/2\alpha_0 \times (\gamma\mu_0 M_s k_{\max}/8\pi)^2 \times (d/f)^2$, with μ_0 the vacuum permeability, and $k_{\max} = \pi/w$ the upper limit of the transverse spin wave vector $k_{\parallel}$ that can be excited by a waveguide with inner conductor width w. Following this dependence the measured α_{eff} should decrease with increasing precession frequency and thus with applied static field. Such dependence is however not observed in Fig. 2(b).

As pointed out by Counil *et al.*[13] nonlinear spin wave excitation results in a more complex time response of M given by

$$M(t) \cong \int_{\omega_0}^{\omega_{\mathrm{MAX}}} e^{-(i\omega+1/\tau)t} d\omega \cong \frac{\sin(\Delta\omega t)}{t} \times e^{-t/\tau} \times \cos([\omega_0 + \Delta\omega]t), \tag{2}$$

where $\Delta\omega$ is the frequency shift induced by the spin waves and ω_0 is the resonance angular frequency derived from Kittel's formula. Considering the long wavelength limit $k_{\parallel}d \ll 1$ the dispersion relation of spin waves propagating orthogonally to the magnetization for a thin film of thickness d is[20] $\omega(k) = \omega_0 \times \sqrt{1 + (\gamma\mu_0 M_s/2\omega_0)^2 \times (2k_{\parallel}d)}$ and the frequency shift $\Delta\omega$, can be written as $\Delta\omega(k) = 1/2[\omega(k) - \omega_0] \cong (\gamma\mu_0 M_s/2)^2 \times (k_{\parallel}d/2\omega_0)$.

As described before experimental determination of α_{eff} is done by fitting the time resolved data by a damped sinusoid. When assuming such fitting for a time resolved precession according to Eq. (2) together with the given thickness dependent frequency shift $\Delta\omega$ due to spin wave generation, the increase in the measured effective damping α_{eff} with thickness can be computed. The such derived thickness dependence of the effective damping for our experimental geometry (with $w = 50$ μm) is given by the blue triangles in Fig. 3. Obviously the increase in α_{eff} by nonlinear spin wave excitation is by far too small to explain the experimental findings and nonlinear spin wave generation can be ruled out as an origin of the observed increase in the effective damping.

Note that the reported thickness dependence of the effective damping parameter significantly differs from those observed in ferromagnetic metals like, e.g., permalloy: while Schneider *et al.*[19] observed an increase in the intrinsic Gilbert damping parameter α_0 with increasing film thickness Council *et al.*[13] and Ingvarsson *et al.*[10] found a decrease in α_0 with increasing thickness for the same material. In the latter case the increase in α_0 with decreasing d was ascribed to a dominating effect of the film surfaces on the damping (e.g., due to surface roughness) which was also correlated with an increased resistivity of the thinner films. In contrast Schneider *et al.*[19] suggest that their observed increasing thickness dependence of α_0 could be related to a different magnetostriction of their films in comparison to the permalloy thin films used, e.g., by Counil *et al.*[13] Although perfect permalloy ideally shows no magnetostriction the occurring differences of the actual Ni–Fe composition of the deposited films could result in an effective magnetostriction of either positive or negative sign. A consecutive study of the magnetization dynamics of thin films of different Ni–Fe alloys showed that α_0 can be modified by more than 100% by changing the Ni-to-Fe ratio.[21] It was found that a negative magnetostriction coefficient ($\lambda_s < 0$) results in a larger damping than a positive one ($\lambda_s > 0$). The abovementioned thickness increase in the Gilbert damping could thus be due to a decreasing magnetostriction with film thickness, as observed in magnetostriction studies of NiFe and CoFe thin films.[22]

Magnetostriction measurements of bulk magnetite reveal a magnetostriction coefficient along the $\langle 100 \rangle$ direction of $\lambda_{100}^{Fe_3O_4} \sim -19.5 \times 10^{-6}$ comparable to those observed for Ni (Ref. 23) and Fe.[24] Unfortunately, to the best of our knowledge, magnetostriction measurements of magnetite thin films are not available and the respective thickness dependence is not known. Here, only a decreasing magnetostriction with increasing film thickness could explain our experimental findings.

Another possible origin could be related to the presence of the so called antiphase boundaries (APBs), which are growth defects resulting from mismatch between the periodicity of the film and the substrate as well as from the difference in rotational symmetries between both. Because the magnetic exchange interaction depends on the distance, the angle, the spin and the electronic configuration of neighboring magnetic moments, there can appear, across the boundary, magnetic interactions that are not present in bulk Fe_3O_4 which will be strongly dependent on the substrate. However, the influence of APBs on α_{eff} has not yet been investigated. Note that in general the density of APBs in magnetite thin films on MgO is expected to decrease with thickness.[25] Therefore, only an increase in α_{eff} with decreasing density of APBs would result in the observed thickness dependence which is quite unlikely considering the lattice defect origin of APBs. However, APBs also contribute to the strain in magnetite thin films.[26] Such strain could also influence magnetostriction[27] and hence modify α_{eff} as a function of film thickness as discussed above.

V. CONCLUSION

In summary, we have investigated the thickness dependence of the magnetization dynamics in high quality epitaxial Fe_3O_4/MgO thin films by inductive measurements. For this, PIMM and VNA-FMR measurements were carried out. Our measurements reveal an upper limit for the intrinsic Gilbert damping parameter of $\alpha_0 \leq 0.0365$ which is significantly lower than previously found for Fe_3O_4 thin films on GaAs.[9] Such low damping together with GHz precession frequencies could enable fast future magnetite based spintronic devices. With increasing film thickness up to 100 nm a strong increase in the effective damping up to about 0.2 is observed. The origin of this effect remains subject of speculation. However, its future understanding could enable the growth of magnetite thin films and nanoparticles having an effective damping specifically tailored to the needs of the given application.

1. E. Snoeck, V. Serin, R. Fourmeaux, Z. Zhang, and P. P. Freitas, J. Appl. Phys. **96**, 3307 (2004).
2. P. J. van der Zaag, P. J. H. Bloemen, J. M. Gaines, R. M. Wolf, P. A. A. van der Heijden, R. J. M. van de Veerdonk, and W. J. M. de Jonge, J. Magn. Magn. Mater. **211**, 301 (2000); C. H. Tsang, R. E. Fontana, T. Lin, D. E. Heim, B. A. Gurney, and M. L. Williams, IBM J. Res. Dev. **42**, 103 (1998); C. Park, J.-G. Zhu, Y. Peng, D. E. Laughlin, and R. M. White, IEEE Trans. Magn. **41**, 2691 (2005).
3. R. Hiergeist W. Andrä, N. Buske, R. Hergt, I. Hilger, U. Richter, and W. Kaiser, J. Magn. Magn. Mater. **201**, 420 (1999).
4. S. Choi, K.-S. Lee, K. Y. Guslienko, and S.-K. Kim, Phys. Rev. Lett. **98**, 087205 (2007); V. E. Demidov, S. O. Demokritov, K. Rott, P. Krzysteczko, and G. Reiss, Appl. Phys. Lett. **92**, 232503 (2008); S. Neusser and D. Grundler, Adv. Mater. **21**, 2927 (2009).
5. S. Trudel, O. Gaier, J. Hamrle, and B. Hillebrands, J. Phys. D: Appl. Phys. **43**, 193001 (2010).
6. P. A. A. van der Heijden, M. G. van Opstal, C. H. W. Swüste, P. H. J. Bloemen, J. M. Gaines, and W. J. M. de Jonge, J. Magn. Magn. Mater. **182**, 71 (1998).
7. B. Aktas, Thin Solid Films **307**, 250 (1997).
8. L. McGuigan, R. C. Barclie, R. G. S. Sofin, S. K. Arora, and I. V. Shvets, Phys. Rev. B **77**, 174424 (2008).
9. C. Bunce, J. Wu, Y. X. Lu, Y. B. Xu, and R. W. Chantrell, IEEE Trans. Magn. **44**, 2970 (2008).
10. S. Ingvarsson, L. Ritchie, X. Y. Liu, G. Xiao, J. C. Slonczewski, P. L. Trouilloud, and R. H. Koch, Phys. Rev. B **66**, 214416 (2002).
11. Y. X. Lu, J. S. Claydon, Y. B. Xu, S. M. Thompson, K. Wilson, and G. van der Laan, Phys. Rev. B **70**, 233304 (2004).
12. T. J. Silva, C. S. Lee, T. M. Crawford, and C. T. Rogers, J. Appl. Phys. **85**, 7849 (1999).
13. G. Counil, J.-V. Kim, T. Devolder, C. Chappert, K. Shigeto, and Y. Otani, J. Appl. Phys. **95**, 5646 (2004).
14. D. T. Margulies, F. T. Parker, M. L. Rudee, F. E. Spada, J. N. Chapman, P. R. Aitchison, and A. E. Berkowitz, Phys. Rev. Lett. **79**, 5162 (1997).
15. S. K. Arora, H. C. Wu, R. J. Choudhary, I. V. Shvets, O. N. Mryasov, H. Yao, and W. Y. Ching, Phys. Rev. B **77**, 134443 (2008).
16. S. Serrano-Guisan, K. Rott, G. Reiss, and H. W. Schumacher, J. Phys. D: Appl. Phys. **41**, 164015 (2008).
17. J. Miltat, G. Albuquerque, and A. Thiaville, Top. Appl. Phys. **83**, 1 (2002).
18. H. G. Oswin and M. Cohen, , J. Electrochem. Soc. **104**, 9 (1957); M. Cohen, Can. J. Chem. **37**, 286 (1959).
19. M. L. Schneider, T. Gerrits, A. B. Kos, and T. J. Silva, Appl. Phys. Lett. **87**, 072509 (2005).
20. C. Mathieu, J. Jorzick, A. Frank, S. O. Demokritov, A. N. Slavin, B. Hillebrands, B. Bartenlian, C. Chappert, D. Decanini, F. Rousseaux, and E. Cambril, Phys. Rev. Lett. **81**, 3968 (1998).
21. R. Bonin, M. L. Schneider, T. J. Silva, and P. J. Nibarger, J. Appl. Phys. **98**, 123904 (2005).
22. C.-Y. Hung, M. Mao, S. Funada, T. Schneider, L. Miloslavsky, M. Miller, C. Qian, and H. C. Tong, J. Appl. Phys. **87**, 6618 (2000).
23. A. Herpin, *Théorie du Magnétisme* (Bibliothèque des Sciences et Techniques Nucléaires, Saclay, 1968).
24. K. Chahara, T. Ohno, M. Kasai, and Y. Kozono, Appl. Phys. Lett. **63**, 1990 (1993).
25. W. Eerenstein, T. T. M. Palstra, T. Hibma, and S. Celotto, Phys. Rev. B **68**, 014428 (2003); D. T. Margulies, F. T. Parker, F. E. Spada, R. S. Goldman, J. Li, R. Sinclair, and A. E. Berkowitz, *ibid.* **53**, 9175 (1996); W. Eerenstein, T. T. M. Palstra, and T. Hibma, *ibid.* **66**, 201101(R) (2002).
26. S. K. Arora, R. G. S. Sofin, I. V. Shvets, and M. Luysberg, J. Appl. Phys. **100**, 073908 (2006).
27. L. W. McKeehan and P. P. Cioffi, Phys. Rev. **28**, 146 (1926).